Eur. Phys. J. C (2020) 80:803
https://doi.org/10.1140/epjc/s10052-020-8388-6

THE EUROPEAN PHYSICAL JOURNAL C

Regular Article - Theoretical Physics

Subleading EW corrections and spin-correlation effects in $t\bar{t}W$ multi-lepton signatures

Rikkert Frederix[a], **Ioannis Tsinikos**[b]

Theoretical Particle Physics, Department of Astronomy and Theoretical Physics, Lund University, Sölvegatan 14A, 223 62 Lund, Sweden

Received: 2 June 2020 / Accepted: 22 August 2020 / Published online: 1 September 2020

Abstract Recently a slight tension between data and predictions has been reported in $t\bar{t}W$ production by both the CMS and ATLAS collaborations. We revisit the theoretical predictions for this process, focussing on the following two effects. We disentangle various effects that lead to asymmetries among the leptonic decay products of the (anti-)top quarks and W bosons, for which we find that the spin correlations in the top-quark pair are the dominant source. We also discuss the impact of the large, formally subleading, electroweak corrections to $t\bar{t}W$ production at the LHC. We find that this effect changes the $t\bar{t}W$ cross section significantly in the signature phase-space regions, and should therefore be included differentially in the theory to data comparisons.

1 Introduction

With the 13 TeV LHC run, both ATLAS and CMS collaborations have measured the $t\bar{t}V(V = Z, W)$ cross sections. These processes are studied either independently [1,2] or as irreducible backgrounds to $t\bar{t}H$ (multilepton) searches [3,4]. In both cases a slight tension between theoretical predictions and data is observed for $t\bar{t}W$ production, with the data suggesting a somewhat larger cross section than Standard Model predictions. This slight tension between Standard Model predictions and data warrants further study of this process from both the experimental and the theoretical sides.

At the production level the $t\bar{t}W$ process has recently been studied in detail at the complete-NLO accuracy [5]. In this work it was pointed out that the subleading EW corrections result in a $\sim$10% increase of the total cross section. This large contribution is due to the opening of $tW \to tW$ scattering diagrams, which are also studied in detail in [6] within a BSM context. The complete-NLO calculation has been matched to soft (threshold) gluon resummation, resulting in the most-accurate predictions for the $t\bar{t}W$ production at the LHC to date [7,8]. Both these works have shown that $t\bar{t}W$, in contrast to $t\bar{t}Z$ and $t\bar{t}H$, does not become less sensitive to the scale choices even when including the resummation at NNLL accuracy. In other words, including the all-order soft-gluon resummation does not significantly decrease the theoretical uncertainties. This can predominantly be attributed to the absence of gluon-induced channels at LO; the latter only appear at higher orders and give sizeable contributions to the cross section. Since they do not contribute at LO they are not considered in the resummation frameworks of Refs. [7,8]. Incidentally, since the gg channels only open at NNLO accuracy there is a large $t\bar{t}$ asymmetry of $\sim$3% in $t\bar{t}W$ production [7,9,10].

By including the decay of $t\bar{t}W$, this accuracy cannot be maintained due to the complexity of the calculation. It is shown in Ref. [9] that the presence of the W boson polarises the initial quark-line and in turn the final $t\bar{t}$ pair. The emerged lepton asymmetry is of $\sim -13\%$ at NLO in QCD and has consequences on the final lepton pseudo-rapidity distributions. Therefore it affects the fiducial region of the final multi-lepton signatures depending on the applied cuts. Furthermore the subleading EW $tW \to tW$ scattering contributions are governed by different kinematics and as a result a non-flat effect is expected in the fiducial region.

The largest tension for $t\bar{t}W$ is found when it enters as the main background in the $t\bar{t}H$ multi-lepton analyses. It is reported in [3] that the normalisation factor for the $t\bar{t}W$ background in the two same sign lepton signature is $1.56^{+0.30}_{-0.28}$ (at low jet multiplicity) and in the three lepton signature is $1.68^{+0.30}_{-0.28}$, which indicate in both cases the lower theoretical $t\bar{t}W$ cross section in comparison with the data. These multi-lepton signatures is what we focus on in this work. We study all effects that lead to lepton asymmetries in detail. We further study contributions that have not been yet taken under consideration in the fiducial region: for the first time,

[a] e-mail: rikkert.frederix@thep.lu.se

[b] e-mail: ioannis.tsinikos@thep.lu.se (corresponding author)

we include the subleading EW corrections in a consistent matching to the parton shower. The latter allows us to investigate the effects from these large corrections differentially in the fiducial region relevant to the $t\bar{t}H$ multi-lepton signatures.

The structure of this paper is the following: in Sect. 2 we discuss the input parameters, describe the framework of the calculation and we define the experimental fiducial region under study. In Sect. 3 we discuss the main subleading EW and spin-correlation effects on differential distributions and their impact on measurements. We present our conclusions in Sect. 4.

2 Input parameters and calculation setup

We consider the NLO corrections to both $pp \to t\bar{t}W^+$ and $pp \to t\bar{t}W^-$ production in the fiducial region following the ATLAS analysis of Ref. [3]. The calculation is performed within the MadGraph5_aMC@NLO [11] framework including the automation of the EW calculations [12]. In accordance with the notation of [5] we define for any observable the QCD and subleading EW ($\mathrm{EW_{sub}}$) perturbative orders as following:

$$\begin{aligned}\Sigma_{\mathrm{QCD}} &= \alpha_s^2\alpha\,\Sigma_{3,0}^{t\bar{t}W} + \alpha_s^3\alpha\,\Sigma_{4,0}^{t\bar{t}W} \\ &= \Sigma_{\mathrm{LO}_1} + \Sigma_{\mathrm{NLO}_1} \\ \Sigma_{\mathrm{EW_{sub}}} &= \alpha^3\,\Sigma_{3,2}^{t\bar{t}W} + \alpha_s\alpha^3\,\Sigma_{4,2}^{t\bar{t}W} \\ &= \Sigma_{\mathrm{LO}_3} + \Sigma_{\mathrm{NLO}_3}\,. \end{aligned} \tag{2.1}$$

We perform the calculation in the 5 Flavour Scheme, setting the factorisation and renormalisation scales to $\mu = \frac{H_T}{2}$ and using the NLO PDF4LHC PDF sets, with associated value for the strong coupling. As input parameters we use

$$\begin{aligned} &m_t = 173.34\,\mathrm{GeV}, \quad m_Z = 91.1876\,\mathrm{GeV} \\ &a_{EW} = 1/132.232, \quad G_\mu = 1.16639\times 10^{-5}\,\mathrm{GeV}^{-2}. \end{aligned} \tag{2.2}$$

The top quarks are decayed to b quarks and W-bosons with a branching ratio of 100%. The W bosons are decayed inclusively, i.e. both the prompt W bosons and the ones induced by the top quark decays are allowed to decay to quarks and leptons. Unless stated otherwise, all these decays are realised within the MadSpin framework [13] in order to fully keep the (LO) spin correlations.

We match the calculation to the parton shower using the PYTHIA8 framework [14] in the default tune, using MadGraph5_aMC@NLO's build-in MC@NLO matching technique [15,16]. The reason that the $\mathrm{EW_{sub}}$ contribution can be included in the matching to the parton shower is that the perturbative order $\alpha_s\alpha^2$ (the LO_2 in the notation of Ref. [5]) is exactly zero for this process. As a result the $\alpha_s\alpha^3$ order can be considered as pure QCD corrections to the α^3 one.[1] The large $tW \to tW$ scattering enters only in the real-emission diagrams of the Σ_{NLO_3} contributions which are effectively included only at LO accuracy. Therefore, in principle, this contribution could also be included by using a LO merging approach, such as CKKW or MLM [17–19], starting from Σ_{LO_3}. However, these latter approaches require the introduction of a merging scale, which will ultimately remove part of the $tW \to tW$ scattering contribution, and that will hamper the accuracy of the inclusive sample.[2] Furthermore, these approaches also rely on the fact that the LO_2 is exactly zero. For this reason one is able to merge Σ_{LO_3} with the tree-level contributions of Σ_{NLO_3} consistently. Consequently, it will not be possible to include additional jets in the merging (e.g. $t\bar{t}Wjj$ tree-level contributions of order $\alpha_s^2\alpha^3$), since the tree-level contributions of order $\alpha_s^2\alpha^2$ (Σ_{NLO_2} in the notation of [5]) are non-zero. For these reasons, an MLM or CKKW merging approach to including $tW \to tW$ scattering into an inclusive $t\bar{t}W$ sample is suboptimal as compared to an MC@NLO matching.

In order to understand the spin-related and the subleading EW effects, before applying any particle selection or cuts, we define the inclusive (no cuts) signature. Furthermore, once specified, we select only events for which the top-quark pair decays to a muon pair and the associated W boson to an electron(positron), using MC-truth. This is done only in order to pin down the origin of various effects and for our final results the decays are inclusive. For the signal-region definitions we start with the selection and the cuts, for which we follow the experimental analysis of [3]. We identify the particles as following:

$$\begin{aligned} \text{Electrons:}\quad & p_T(e) \geq 10\,\mathrm{GeV}, \quad |\eta(e)| \leq 2.47\ (2 \text{ for tight}) \\ \text{Muons:}\quad & p_T(\mu) \geq 10\,\mathrm{GeV}, \quad |\eta(\mu)| \\ & \leq 2.5\ (\text{same for tight}) \\ \text{jets:}\quad & k_T = -1, \quad R = 0.4, \quad pT(j) \\ & \geq 25\,\mathrm{GeV}, \quad |\eta(j)| \leq 2.5. \end{aligned} \tag{2.3}$$

The τ leptons are allowed to decay within the shower and we identify the hadronic τ_h. We reject the jets that have $\Delta R(j,e) \leq 0.3$ or $\Delta R(j,\tau_h) \leq 0.3$. Furthermore we discard the muons that lie within $\Delta R(j,\mu) \leq 0.4$.

[1] What are usually called the EW-corrections, i.e. the $\alpha_s^2\alpha^2$ perturbative order (a.k.a. NLO_2), are not included here. These EW corrections change the cross section by about $\sim -4\%$ [12,20].

[2] Moreover, these approaches have never been validated for processes where after including higher multiplicity contributions the cross section of the inclusive sample increases by about an order of magnitude due to the opening of new channels and might therefore not work out-of-the-box.

With this particle selection we define the two following signatures: the same sign dilepton (2ssℓ) and the three lepton (3ℓ) channels. In both cases we require at least two jets and at least one b-tagged jet and zero hadronic τ_h's. For the 2ssℓ signature we require exactly two tight same sign leptons with $p_T(\ell) \geq 20$ GeV. Furthermore for the same flavor (SF) pairs we apply the $m(\ell\ell) \geq 12$ GeV condition. For the 3ℓ signature we ask exactly three leptons, two tight same sign (SS) with $p_T(\ell) \geq 15$ GeV and one opposite sign (OS) with $p_T(\ell) \geq 10$ GeV. For the SFOS pairs we ask $m(\ell^+\ell^-) \geq 12$ GeV, $|m(\ell^+\ell^-) - m_Z| \geq 10$ GeV and for the 3-lepton system $|m(\ell\ell\ell) - m_Z| \geq 10$ GeV.

In PYTHIA8 we include hadronisation, the QED shower (we include the photons in the jets) and the multiparton interactions (underlying event). However, we do not consider any misidentification or identification inefficiencies for the jets or the leptons.

3 Results

Having defined the selection criteria for the particles and the events we proceed now by pointing out the importance of the spin correlations and thereafter showing the effect of the EW_{sub} contributions. In particular, we focus on the jet-multiplicity cross sections, since that is shown by the ATLAS collaboration in Ref. [3] (both with prefit and postfit signal+background contributions). However, since the data has not been unfolded, we cannot directly compare to it. On the other hand, we can study this distribution at the theoretical level to see firstly whether and how it is shaped by the spin correlations and secondly if the EW_{sub} effects considered in this work might have a significant influence on the ATLAS analysis.

3.1 Asymmetries

The effects described in the present section are already included in the modern MC simulations. Nevertheless, they are never disentangled in such detail in order to scrutinise their impact and understand their contribution to the final signatures. A separation of these effects, as we will describe in this section, reveals non trivial partial cancellations between them and shows the dependence of the cross section in the fiducial region on the polarisation of the top-quark pair. Phenomenologically this information gives an insight to various future BSM analyses e.g. in a stop pair (spin zero) production in association with a W boson, in a modification of the $V-A$ structure of the W-boson decays or in an EFT analysis. Depending on the specific BSM scenario, only part of these components will be affected, so one can either a priori estimate or a posteriori explain the BSM effects. For this reason, in the first part of this section we select a specific leptonic decay mode for $t\bar{t}W$ so that we can identify the origin of the final particles. After describing these effects, we move to the second part, where we study their consequences as a total to the multi-lepton signatures, without constraining the decay modes of $t\bar{t}W$.

Moving to the first part, the asymmetries in the lepton decay products of the $t\bar{t}W^+$ and $t\bar{t}W^-$ can be attributed to separate origins, which are depicted in Figs. 1 and 2 and described in what follows.

Only for this part, in order to track the origin of the leptons, we have selected the events where the top quark pair decays to muons and the associated $W^-(W^+)$ to electrons(positrons). Furthermore we restrict the analysis only to the QCD shower within PYTHIA8 without applying any cuts or selections. We denote the origin of each lepton with a subscript. In Fig. 1 we show the various effects on the decay products of the top pair, whereas in Fig. 2 of the associated W boson. In both these figures the prediction that corresponds to the modern MC simulations is the one that includes all these effects, i.e. the blue line. We now separate these effects on the lepton asymmetries:

- The $t\bar{t}W^+$ production is induced predominately by the $u\bar{d} + c\bar{s}$ luminosity, while $t\bar{t}W^-$ one mostly by $\bar{u}d + \bar{c}s$. This results in the total cross section for top pairs associated with the positively charged vector boson to be about a factor two larger than the negatively charged vector boson. Moreover, $t\bar{t}W^+$ typically probes larger Björken x values than $t\bar{t}W^-$ resulting, on average, in harder and more forward leptons in the former as compared to the latter. This effect in Figs. 1 and 2 is defined as 'PDF' and it affects both the top pair and the W associated decay products. All the other effects are added on top of this. Since in Fig. 1 there is no distinction made for muons coming from $t\bar{t}W^+$ versus muons coming from $t\bar{t}W^-$, there is no PDF effect visible here. On the other hand, for the electron/positron coming from the associated W-boson decay this distinction is made, and therefore the PDF effect is clearly visible in the lower two plots of Fig. 2, with the positron from the $t\bar{t}W^+$ process being at larger rapidities and harder than the electron from the $t\bar{t}W^-$ process.
- The second cause for differences between the leptonic decay products is due to the Central-Peripheral asymmetry in the top pairs [21–25]. This effect only enters at NLO in QCD, and was first studied for top pair production at the Tevatron, where it showed as a charge asymmetry [26–29]. Compared to $pp \to t\bar{t}$ production, requiring the associated W-boson increases the asymmetry [9]. In Fig. 1 this is denoted as 'A_C^{QCD}'. It results in about 3-5% differences in the pseudo-rapidity of the lepton coming from the top decay versus the one coming from the

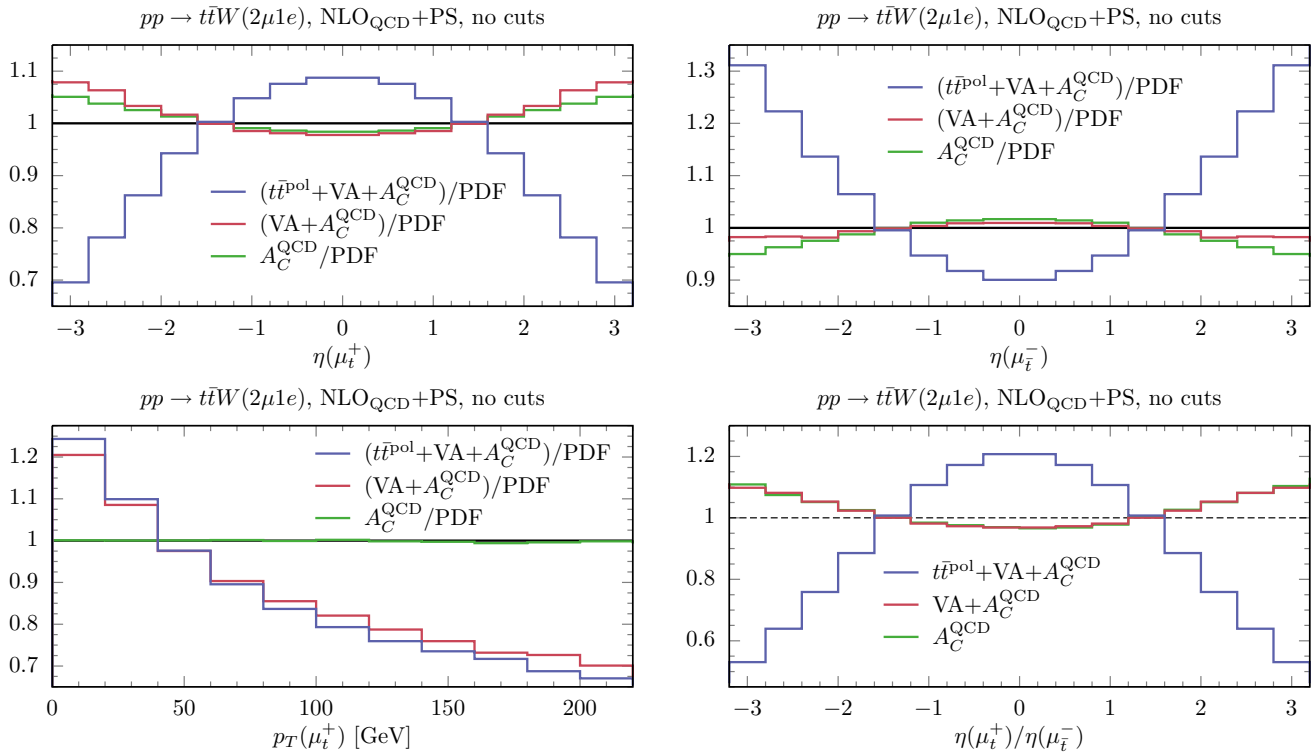

Fig. 1 Origin of asymmetries in top pair decay products. The muons in these plots exclusively originate from the top-quark pair. The sum of these effects (blue line) is included in the modern MC simulations

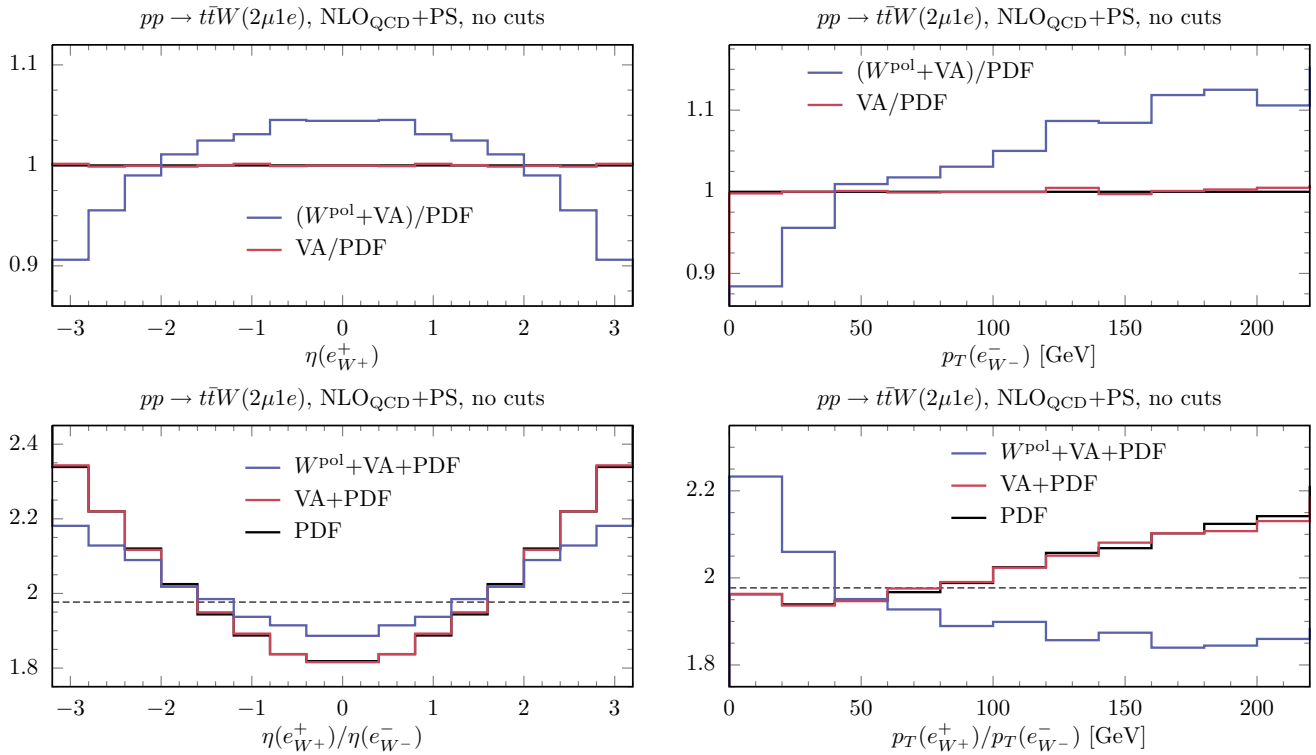

Fig. 2 Origin of asymmetries in W associated decay products. The electrons (positrons) in these plots originate exclusively from the $W^-(W^+)$ associated boson. The sum of these effects (blue line) is included in the modern MC simulations

anti-top decay (pseudo-rapidity insets in Fig. 1). It has a negligible effect on the corresponding p_T distributions (Fig. 1).

- The third effect that could lead to asymmetries among the leptonic W-boson decays is the $V-A$ structure of the W-boson couplings. This is denoted in Figs. 1 and 2 as 'VA' effects. While these effects are not there for the decays of the associated W-boson (Fig. 2), the $V-A$ coupling structure in the three-body decays of the top and the anti-top quarks results in a large asymmetry between the charged leptons and the neutrinos. They do affect the charged leptons from the top identically to the ones from the anti-top, and therefore do not generate an asymmetry in the visible lepton decays (Fig. 1). Concerning the leptons originating from the associated W boson, the 'VA' effects are present once the spin correlations of the associated W boson (denoted as W^{pol}) are taken into account. In this case, as shown in Fig. 2, the effects are different between the associated W^+ and W^- and affect both the transverse momentum and pseudo-rapidity ratios.
- The most important source for the asymmetry is the top-quark pair polarization. Due to the associated W, these correlations are rather sizeable and significantly alter the shapes of the rapidities of the leptonic decays of the top quark as compared to the leptonic decays of the anti-top quark (denoted as $t\bar{t}^{\text{pol}}$ in Fig. 1). These effects result in a charge asymmetry of the leptons that reaches about $-13-15\%$ at the cross section level [9]. As shown in Fig. 1 in the pseudo-rapidity ratio these effects are between $\sim+20\%$ (central region) and $\sim-40\%$ (peripheral region).
- The final source of asymmetry is due to the NLO electroweak corrections being of different size for $t\bar{t}W^+$ and $t\bar{t}W^-$ production. This is a negligible effect of $\sim$0.5% [7] and not considered in this work.

Having described the different roles of the various sources of asymmetries, we now move to the second part, where we adopt the realistic setup described in Sect. 2, i.e. including QED-shower, hadronisation and underlying event, without any restrictions to the decay modes. We first note that the consequences of these asymmetries on the $t\bar{t}W$ background in the $t\bar{t}H$ multi-lepton signatures are significant even at the cross section level. Since the largest of these effects are the spin correlations, we compare the effect of these on the inclusive level as well as on the 2ssℓ and 3ℓ signatures. As a first step, at the inclusive level (no cuts), we show in the two upper plots of Fig. 3 that these effects are not altered by adopting the aforementioned realistic setup. As one can see from Figs. 1 and 2 and the upper two plots of Fig. 3, the spin correlations allow more ℓ^+'s than ℓ^-'s within the selection criteria (Eq. 2.3). This, in combination with the fact that there are more ℓ^+'s produced than ℓ^-'s due to the $t\bar{t}W^+$ cross section being larger than the $t\bar{t}W^-$ one by a factor of $\sim$2, increases the fiducial cross section of $t\bar{t}W$ production in both the 2ssℓ and 3ℓ signatures. This can also be seen in the two lower plots of Fig. 3, where we show the jet multiplicities with and without the spin-correlation effects for the 2ssℓ and 3ℓ signatures in the left and right plots, respectively. The increase in the cross section due to the spin correlations between the top and the anti-top is about 10% and slightly larger for the lower-multiplicity bins as compared to the higher ones.

Alternatively, the effects of the spin correlations can be presented in the value of the charge ratio $\sigma_{t\bar{t}W^+}/\sigma_{t\bar{t}W^-}$ for the various signatures. This is shown in Table 1. In this table we show the ratio for the total cross section and bin by bin for the jet multiplicity in both signatures. As a reference and in accordance with Fig. 3, we also show the same ratio before any selections or cuts (no cuts) as well as before the spin-correlation effects (no spin) are taken into account. We further show the double ratios between spin and no spin in all three cases. As expected, the inclusive result (before any selections or cuts) is not affected by the spin correlations. Without including the latter, in both signatures the charge ratio decreases from 1.977 to 1.84. This is mostly due to the decrease of the $\eta(e^+)/\eta(e^-)$ ratio in the central pseudo-rapidity region due to the PDF effect, as shown in Fig. 2. By including the spin-correlation effects the charge ratio in the 2ssℓ signature increases, and accidentally agrees within the uncertainties with the inclusive result. In the 3ℓ signature the ratio also increases, but less. This difference, which is directly shown in the double ratios, is due to the strong preference of the 2ssℓ signature to the positively charged lepton pair as shown in the pseudo-rapidity distributions of Fig. 1 and which we will now elaborate on in more detail.

In the 2ssℓ signature it is more often that the anti-top (as compared to the top) decays hadronically within this signal region. This is because $\sigma(t\bar{t}W^+) > \sigma(t\bar{t}W^-)$ and the (potential) ℓ^+ from top is more central than the (potential) ℓ^- from the anti-top due to spin correlations. This results to a larger increase of the charge ratio due to spin correlations as compared to the 3ℓ signature, where all three massive particles need to decay (semi-)leptonically. Hence, for the 3ℓ signature also the more-forward ℓ^- from the anti-top needs to be within the selection criteria, resulting in a smaller increase due to spin correlations than for the 2ssℓ signature. Besides this, also the 'PDF' affects the 2ssℓ signature differently from the 3ℓ one. In both these signatures the associated W boson decays leptonically and the 'PDF' effect described in Sect. 3.1 affects them in the same way. This is not true for the top-quark pair decay products. In the 3ℓ signature both the top and anti-top quarks decay semi-leptonically, therefore no extra asymmetry is induced from 'PDF' effect. However in the case of 2ssℓ signature there is an extra asymmetry induced due to the fact that for the positively charged lepton pair both leptons will be

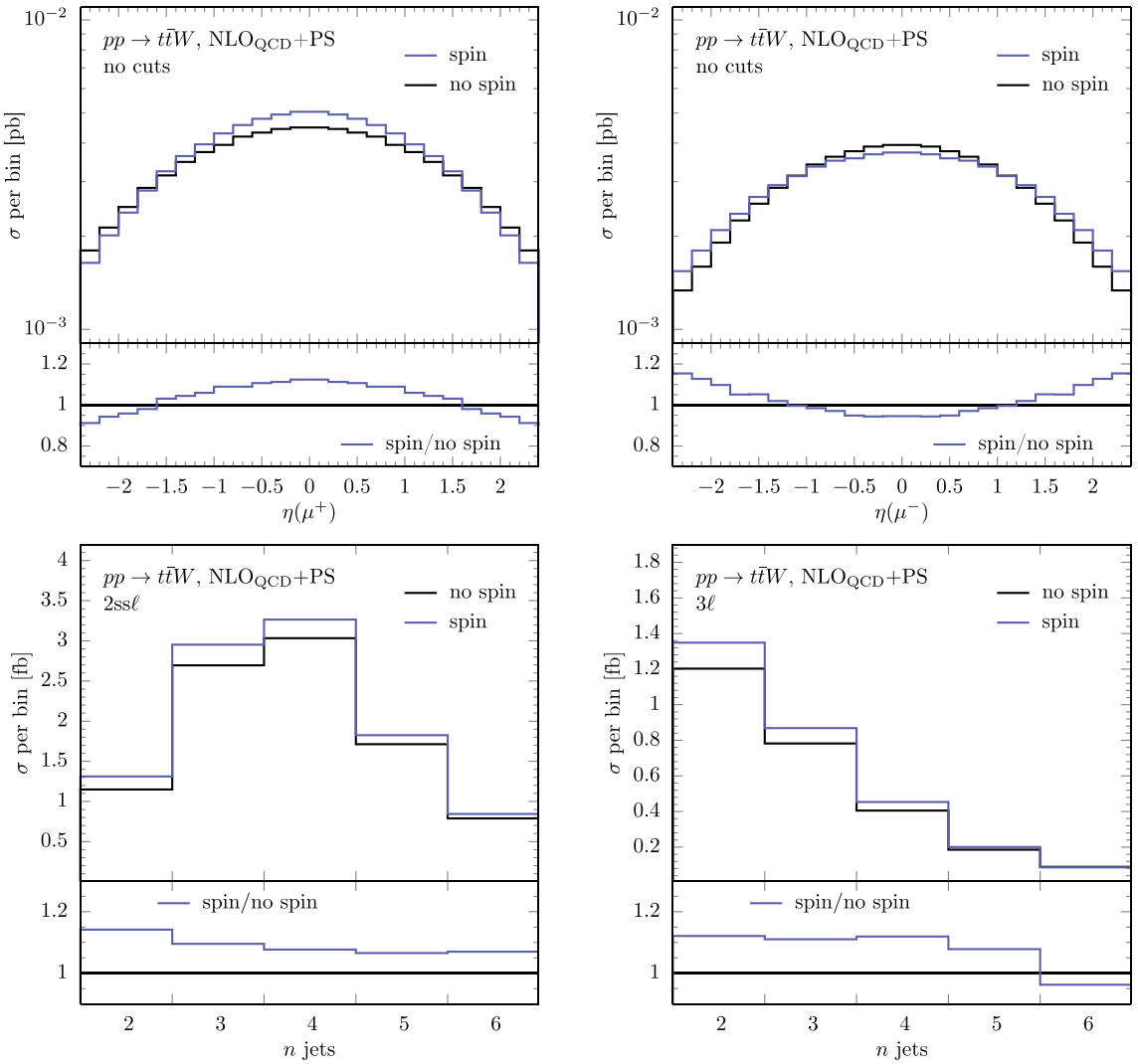

Fig. 3 Spin correlation effects on lepton pseudo-rapidities and jet multiplicities. The muons in the upper plots are the leading in p_T regardless their origin

Table 1 Charge ratio $\sigma_{t\bar{t}W^+}/\sigma_{t\bar{t}W^-}$ and double ratios (spin over no spin) in different signatures. The scale uncertainties can be taken to be correlated and are therefore of the order of the statistical error (in parantheses) and are not shown

Jet multiplicity:	Inclusive	0	1	2	3	4	5	6
No cuts	1.977(2)	2.88(4)	2.43(1)	2.218(7)	2.087(4)	2.003(3)	1.956(3)	1.916(3)
No cuts-no spin	1.977(1)	2.90(4)	2.45(1)	2.205(7)	2.087(5)	2.003(4)	1.956(3)	1.920(3)
No cuts-double ratio	1.000(1)	0.99(2)	0.992(6)	1.006(5)	1.000(3)	1.000(2)	1.000(2)	0.998(2)
2ssℓ	1.99(2)	–	–	2.30(3)	2.02(2)	1.96(2)	1.94(3)	1.84(4)
2ssℓ-no spin	1.84(1)			1.90(3)	1.84(2)	1.84(2)	1.84(3)	1.72(4)
2ssℓ-double ratio	1.08(1)			1.21(3)	1.10(2)	1.07(2)	1.05(2)	1.07(3)
3ℓ	1.88(2)	–	–	1.89(3)	1.92(4)	1.81(5)	1.83(8)	1.8(1)
3ℓ-no spin	1.84(2)			1.81(3)	1.82(4)	1.86(5)	1.90(8)	1.9(1)
3ℓ-double ratio	1.02(2)			1.04(2)	1.06(3)	0.97(4)	0.96(6)	0.95(7)

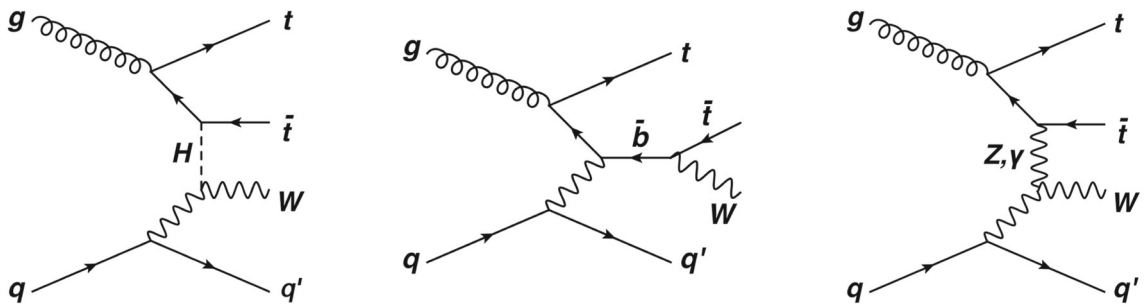

Fig. 4 Dominant representative Feynman diagrams for the $\mathrm{EW}_{\mathrm{sub}}$ contributions in the $\alpha_s\alpha^3$ perturbative order

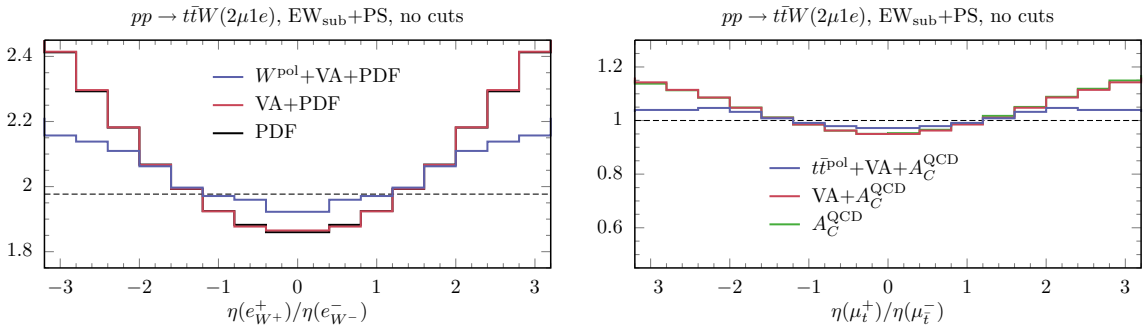

Fig. 5 Origin of asymmetries in W associated (left) and top-quark pair (right) decay products for the $\mathrm{EW}_{\mathrm{sub}}$ perturbative orders

on average harder and more forward (emerging from $t\bar{t}W^+$) as compared to the negatively charged lepton pair (emerging from $t\bar{t}W^-$). Even though this effect is opposite to the one from the top-quark pair spin correlations, the latter is always dominant, resulting in a larger charge ratio for the 2ssℓ as compared to the 3ℓ signatures.

Concerning the jet multiplicity, the charge ratio decreases at the highest jet multiplicities, where the shower effects become important. We have checked that these results do not change significantly once we add the $\mathrm{EW}_{\mathrm{sub}}$ contributions to the NLO QCD, as we will explain in Sect. 3.2. We have also verified that already without misidentifications or identification inefficiencies there is a large migration of events from the 3-lepton decay mode to the 2ssℓ signature (which is included in our results). However this effect is expected to be enhanced in the experimental analyses and there will also be the inverse migration (2-lepton decay mode to 3ℓ signature). Therefore the results presented in Fig. 3 and Table 1 are expected to be sensitive to these effects and should be reconsidered with full detector simulation.

3.2 Subleading EW contributions

Having understood in Sect. 3.1 the origin of the lepton asymmetries and their impact on the different final signatures we proceed to the discussion on the $\mathrm{EW}_{\mathrm{sub}}$ contributions, as defined in Eq. 2.1. It is shown in Ref. [12] and discussed in detail in Ref. [5] that the ∼10% the $\mathrm{EW}_{\mathrm{sub}}$ contributions originate almost exclusively from the $\alpha_s\alpha^3$ perturbative order (the NLO_3 in the notation of Ref. [5]). The dominant representative diagrams of this contribution are shown in Fig. 4. These contributions are qg initiated with different structure w.r.t. the $q\bar{q}$ initiated contributions that cause the large lepton asymmetries already at LO. Therefore the presence of the W boson does not result to the same spin correlations for the top pair decay products. This can be seen in the plots in Fig. 5, for which we follow the same setup as for Figs. 1 and 2. Regarding the associated W boson decay products (left plot) the contribution of the various effects is similar to the corresponding ones at NLO in QCD (lower left plot in Fig. 2). However this is not the case for the top-quark pair decay products (right plot). Due to the aforementioned differences of these contributions, the large effect of the top-quark pair spin correlations (lower right plot in Fig. 1) is not there. This last remark shows that the inclusion of the $\mathrm{EW}_{\mathrm{sub}}$ contributions slightly flattens the asymmetries of the top-quark pair leptons. The overall effect is small, since the total contribution from the $\mathrm{EW}_{\mathrm{sub}}$ is only ∼10%. As a result the charge ratio presented in Table 1 is not altered within the given statistical MC errors by the inclusion of the $\mathrm{EW}_{\mathrm{sub}}$ perturbative orders. In the next paragraph we explore the effect

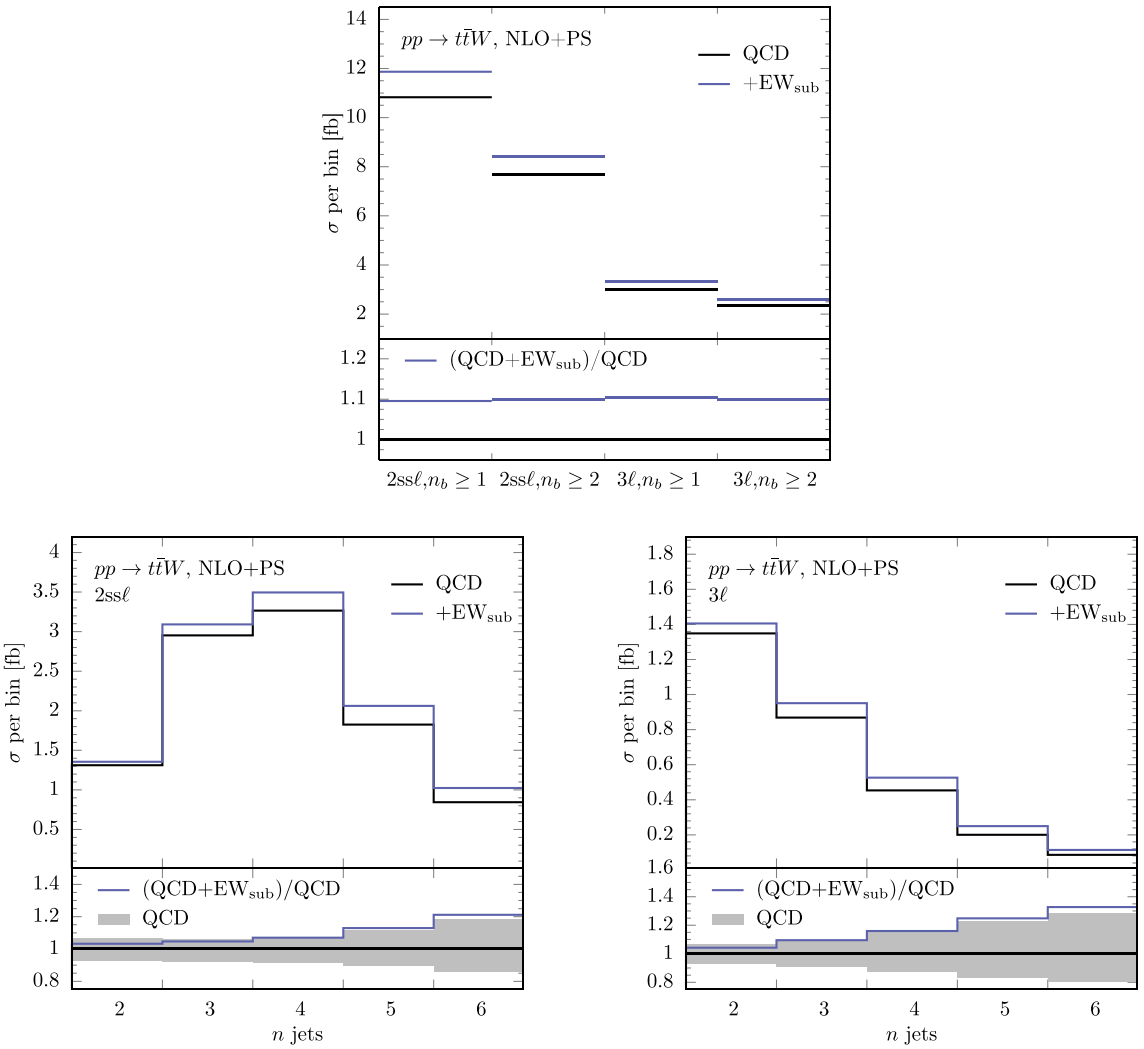

Fig. 6 Effect of the EW$_{\text{sub}}$ contributions on the cross section and the jet multiplicities for the 2ssℓ and 3ℓ signatures

of the EW$_{\text{sub}}$ contributions to the total cross section and the jet multiplicities within the selected signatures.

Starting from the NLO QCD production the inclusion of the EW perturbative orders up to now is done by applying a flat scaling factor 0.96 for the -4% contribution of the $\alpha_s^2\alpha^2$ perturbative order and a 1.09 for the contribution of the EW$_{\text{sub}}$ contributions [3]. In the upper plot of Fig. 6 we start by showing the effect of the latter on the cross sections for both the 2ssℓ and 3ℓ signatures requiring at least one ($n_b \geq 1$) or two ($n_b \geq 2$) b-jets. As shown in the plot, in all the selected signatures there is a 10% effect of the EW$_{\text{sub}}$ contributions in agreement with the aforementioned applied scaling factor. In the lower two plots of Fig. 6 the jet multiplicities in the 2ssℓ and 3ℓ are shown in the left and right plot, respectively. From these plots one can see that the effects from the EW$_{\text{sub}}$ are not flat. In particular, they have a rather small effect in the low jet-multiplicity bins, but are significantly larger in the higher jet-multiplicity bins. Hence, they behave opposite from the spin-correlation effects presented in the lower plots of Fig. 3. In the lower insets, also the scale uncertainties (obtained in the usual way by taking the envelope of the $3 \times 3 = 9$ point variation of the renormalisation and factorisation scales) in the $t\bar{t}W$ production process are shown. The EW$_{\text{sub}}$ are just at the edge of the scale uncertainty band[3]. The main reason for this behaviour at the differential level is the fact that the dominant topologies of the EW$_{\text{sub}}$ contributions (Fig. 4) have an extra parton. As a result, the peaks of the jet multiplicities (lower plots of Fig. 3) are shifted to the right and furthermore the extra parton increases the sources of radiation.

[3] One should keep in mind that, in particular for the larger multiplicities, there is also a significant uncertainty coming from the parton shower modeling, which we have not included here.

4 Conclusions

In this work we discussed two non-negligible effects in $t\bar{t}W$ production: spin correlations in the top-quark pair and the large, formally subleading EW corrections (mainly) induced by $tW \to tW$ scattering. In the current experimental analyses the former is included, whereas the latter is simulated via a flat K-factor. Concerning the spin correlations we disentangled every source of asymmetry relevant to the final signatures. We have shown the partial cancellations between the different sources and that the polarisation of intermediate particles (top pair) has large effects on the final signatures. We further studied and presented, for the first time, the impact of the $\mathrm{EW}_{\mathrm{sub}}$ contributions on the selected signatures within a realistic analysis setup. We have found that both effects enhance the $t\bar{t}W$ background in the 2ssℓ and 3ℓ signal regions of $t\bar{t}H$ production by approximately 10%. However, their effects are not flat in the phase-space. In particular, we considered the cross sections binned in jet multiplicity and found that the spin correlation effects enhance the low jet multiplicities more than high jet multiplicities, and the $\mathrm{EW}_{\mathrm{sub}}$ inducing an opposite effect. However, since the induced differences in shapes are rather different, also the combined effect of spin correlations and $\mathrm{EW}_{\mathrm{sub}}$ contributions is not be flat in phase-space. Hence, we can conclude that both effects are important, and that both effects need to be included in the analysis in a differential manner. For the latter effect, this work shows, for the first time, that this can indeed be done: it is possible to use the default MC@NLO matching, as available in Madgraph5_aMC@NLO, to include the large $\mathrm{EW}_{\mathrm{sub}}$ contributions (which include $tW \to tW$ scattering) within the standard event generation framework.

Acknowledgements This work is done in the context of and supported by the Swedish Research Council under Contract number 2016-05996. IT would like to thank Rohin Narayan for the detailed discussions on the experimental analysis.

Data Availability Statement This manuscript has no associated data or the data will not be deposited. [Authors' comment: There are no data attached for the plots in the paper, because the experimental particle-level unfolded data are not yet public. As a result no direct comparison between our results and experimental data can be done.]

Funded by SCOAP[3].

References

1. M. Aaboud et al. (ATLAS Collaboration), Measurement of the $t\bar{t}Z$ and $t\bar{t}W$ cross sections in proton–proton collisions at $\sqrt{s} = 13$ TeV with the ATLAS detector. Phys. Rev. D **99**(7), 072009 (2019). https://doi.org/10.1103/PhysRevD.99.072009. arXiv:1901.03584 [hep-ex]
2. A.M. Sirunyan et al. (CMS Collaboration), Measurement of the cross section for top quark pair production in association with a W or Z boson in proton–proton collisions at $\sqrt{s} = 13$ TeV. JHEP **1808**, 011 (2018). https://doi.org/10.1007/JHEP08(2018)011. arXiv:1711.02547 [hep-ex]
3. The ATLAS Collaboration, Analysis of $t\bar{t}H$ and $t\bar{t}W$ production in multilepton final states with the ATLAS detector, ATLAS-CONF-2019-045. https://inspirehep.net/files/fe530391c045e7d9b61277532f0b2c00
4. CMS Collaboration, Search for Higgs boson production in association with top quarks in multilepton final states at $\sqrt{s} = 13$ TeV. CMS-PAS-HIG-17-004. https://inspirehep.net/files/02aa157dfabd7beba15deefac195c7ca
5. R. Frederix, D. Pagani, M. Zaro, Large NLO corrections in $t\bar{t}W^{\pm}$ and $t\bar{t}t\bar{t}$ hadroproduction from supposedly subleading EW contributions. JHEP **1802**, 031 (2018). https://doi.org/10.1007/JHEP02(2018)031. arXiv:1711.02116 [hep-ph]
6. J.A. Dror, M. Farina, E. Salvioni, J. Serra, JHEP **01**, 071 (2016). https://doi.org/10.1007/JHEP01(2016)071. arXiv:1511.03674 [hep-ph]
7. A. Broggio, A. Ferroglia, R. Frederix, D. Pagani, B.D. Pecjak, I. Tsinikos, Top-quark pair hadroproduction in association with a heavy boson at NLO+NNLL including EW corrections. JHEP **1908**, 039 (2019). https://doi.org/10.1007/JHEP08(2019)039. arXiv:1907.04343 [hep-ph]
8. A. Kulesza, L. Motyka, D. Schwartländer, T. Stebel, V. Theeuwes, Associated top quark pair production with a heavy boson: differential cross sections at NLO+NNLL accuracy. Eur. Phys. J. C **80**(5), 428 (2020). https://doi.org/10.1140/epjc/s10052-020-7987-6 [hep-ph]
9. F. Maltoni, M.L. Mangano, I. Tsinikos, M. Zaro, Top-quark charge asymmetry and polarization in $t\bar{t}W^{\pm}$ production at the LHC. Phys. Lett. B **736**, 252 (2014). https://doi.org/10.1016/j.physletb.2014.07.033. arXiv:1406.3262 [hep-ph]
10. F. Maltoni, D. Pagani, I. Tsinikos, Associated production of a top-quark pair with vector bosons at NLO in QCD: impact on tt̄H searches at the LHC. JHEP **1602**, 113 (2016). https://doi.org/10.1007/JHEP02(2016)113. arXiv:1507.05640 [hep-ph]
11. J. Alwall et al., The automated computation of tree-level and next-to-leading order differential cross sections, and their matching to parton shower simulations. JHEP **1407**, 079 (2014). https://doi.org/10.1007/JHEP07(2014)079. arXiv:1405.0301 [hep-ph]
12. R. Frederix, S. Frixione, V. Hirschi, D. Pagani, H.-S. Shao, M. Zaro, The automation of next-to-leading order electroweak calculations. JHEP **1807**, 185 (2018). https://doi.org/10.1007/JHEP07(2018)185. arXiv:1804.10017 [hep-ph]
13. P. Artoisenet, R. Frederix, O. Mattelaer, R. Rietkerk, Automatic spin-entangled decays of heavy resonances in Monte Carlo simulations. JHEP **1303**, 015 (2013). https://doi.org/10.1007/JHEP03(2013)015. arXiv:1212.3460 [hep-ph]
14. T. Sjöstrand et al., An introduction to PYTHIA 8.2. Comput. Phys. Commun. **191**, 159 (2015). https://doi.org/10.1016/j.cpc.2015.01.024. arXiv:1410.3012 [hep-ph]
15. S. Frixione, B.R. Webber, Matching NLO QCD computations and parton shower simulations. JHEP **0206**, 029 (2002). https://doi.org/10.1088/1126-6708/2002/06/029. arXiv:hep-ph/0204244
16. S. Frixione, P. Nason, B.R. Webber, Matching NLO QCD and parton showers in heavy flavor production. JHEP **0308**,

007 (2003). https://doi.org/10.1088/1126-6708/2003/08/007. arXiv:hep-ph/0305252
17. M.L. Mangano, M. Moretti, F. Piccinini, M. Treccani, JHEP **01**, 013 (2007). https://doi.org/10.1088/1126-6708/2007/01/013. arXiv:hep-ph/0611129
18. S. Catani, F. Krauss, R. Kuhn, B.R. Webber, JHEP **11**, 063 (2001). https://doi.org/10.1088/1126-6708/2001/11/063. arXiv:hep-ph/0109231
19. J. Alwall, S. Hoche, F. Krauss, N. Lavesson, L. Lonnblad, F. Maltoni, M.L. Mangano, M. Moretti, C.G. Papadopoulos, F. Piccinini, S. Schumann, M. Treccani, J. Winter, M. Worek, Eur. Phys. J. C **53**, 473–500 (2008). https://doi.org/10.1140/epjc/s10052-007-0490-5. arXiv:0706.2569 [hep-ph]
20. S. Frixione, V. Hirschi, D. Pagani, H.-S. Shao, M. Zaro, Electroweak and QCD corrections to top-pair hadroproduction in association with heavy bosons. JHEP **1506**, 184 (2015). https://doi.org/10.1007/JHEP06(2015)184. arXiv:1504.03446 [hep-ph]
21. J.H. Kuhn, G. Rodrigo, Charge asymmetries of top quarks at hadron colliders revisited. JHEP **1201**, 063 (2012). https://doi.org/10.1007/JHEP01(2012)063. arXiv:1109.6830 [hep-ph]
22. W. Hollik, D. Pagani, The electroweak contribution to the top quark forward–backward asymmetry at the Tevatron. Phys. Rev. D **84**, 093003 (2011). https://doi.org/10.1103/PhysRevD.84.093003. arXiv:1107.2606 [hep-ph]
23. W. Bernreuther, Z.G. Si, Top quark and leptonic charge asymmetries for the Tevatron and LHC. Phys. Rev. D **86**, 034026 (2012). https://doi.org/10.1103/PhysRevD.86.034026. arXiv:1205.6580 [hep-ph]
24. M. Czakon, P. Fiedler, A. Mitov, Phys. Rev. Lett. **115**(5), 052001 (2015). https://doi.org/10.1103/PhysRevLett.115.052001. arXiv:1411.3007 [hep-ph]
25. M. Czakon, D. Heymes, A. Mitov, D. Pagani, I. Tsinikos, M. Zaro, Top-quark charge asymmetry at the LHC and Tevatron through NNLO QCD and NLO EW. Phys. Rev. D **98**(1), 014003 (2018). https://doi.org/10.1103/PhysRevD.98.014003. arXiv:1711.03945 [hep-ph]
26. T. Aaltonen et al. (CDF Collaboration), Measurement of the top quark forward–backward production asymmetry and its dependence on event kinematic properties. Phys. Rev. D **87**(9), 092002 (2013). https://doi.org/10.1103/PhysRevD.87.092002. arXiv:1211.1003 [hep-ex]
27. T. Aaltonen et al. (CDF Collaboration), Measurement of the differential cross section $d\sigma/d(\cos\theta t)$ for top-quark pair production in $p-\bar{p}$ collisions at $\sqrt{s}=1.96$ TeV. Phys. Rev. Lett. **111**(18), 182002 (2013). https://doi.org/10.1103/PhysRevLett.111.182002. arXiv:1306.2357 [hep-ex]
28. V.M. Abazov et al. (D0 Collaboration), Measurement of the forward–backward asymmetry in top quark–antiquark production in $p\bar{p}$ collisions using the lepton+jets channel. Phys. Rev. D **90**, 072011 (2014). https://doi.org/10.1103/PhysRevD.90.072011. arXiv:1405.0421 [hep-ex]
29. T.A. Aaltonen et al. (CDF and D0 Collaborations), Combined forward–backward asymmetry measurements in top–antitop quark production at the Tevatron. Phys. Rev. Lett. **120**(4), 042001 (2018). https://doi.org/10.1103/PhysRevLett.120.042001. arXiv:1709.04894 [hep-ex]